

Makara Journal of Science, 20/3 (2016), 135-144
doi: 10.7454/mss.v20i3.6244

MINI-REVIEW

Atomic Ensemble Effects and Non-Covalent Interactions at the Electrode–Electrolyte Interface

Angel Cuesta

Department of Chemistry, School of Natural and Computing Sciences, University of Aberdeen
Meston Road, Aberdeen AB24 3UE, UK

E-mail: angel.cuestaciscar@abdn.ac.uk

Received March 30, 2016 | Accepted August 4, 2016

Abstract

Cyanide-modified Pt(111) electrodes have been recently employed to study atomic ensemble effects in electrocatalysis. This work, which will be briefly reviewed, reveals that the smallest site required for methanol dehydrogenation and formic acid dehydration is composed of three contiguous Pt atoms. By blocking these trigonal sites, the specific adsorption of anions, such as sulfate and phosphate, can be inhibited, thus increasing the rate of oxygen reduction reaction by one order of magnitude or more. Moreover, alkali metal cations affect hydrogen adsorption on cyanide-modified Pt(111). This effect is attributed to the non-covalent interactions at the electrical double layer between specifically adsorbed anions or dipoles and the alkali metal cations. A systematic investigation is conducted on the effect of the concentration of alkali metal cations. Accordingly, a simple model that reproduces the experimental observations accurately and enables the understanding of the trends in the strength of the interaction between M^+ and CN_{ad}^- when moving from Li^+ to Cs^+ , as well as the deviations from the expected trends, is developed. This simple model can also explain the occurrence of super-Nernstian shifts of the equilibrium potential of interfacial proton-coupled electron transfers. Therefore, the model can be generally applied to explain quantitatively the effect of cations on the properties of the electrical double layer. The recently reported effects of alkali metal cations on several electrocatalytic reactions must be mediated by the interaction between these cations and chemisorbed species. As these interactions seem to be adequately and quantitatively described by our model, we expect the model to also be useful to describe, explain, and potentially exploit these effects.

Abstrak

Pengaruh Kumpulan Atom-atom dan Interaksi Non Kovalen pada Antarfasa Elektroda-elektrolit. Elektroda Pt (III) yang dimodifikasi dengan sianida dimanfaatkan untuk mempelajari pengaruh *ensemble* atom pada proses elektroanalisis. Penelitian ini, dibahas secara singkat, menunjukkan bahwa bagian terkecil yang dibutuhkan dalam proses dehidrogenasi metanol dan dehidrasi asam format, terdiri dari tiga atom Pt yang berdekatan. Penelitian ini juga mengungkapkan bahwa dengan menghalangi sisi trigonal tersebut, adsorpsi anion tertentu seperti sulfat dan fosfat dapat dicegah, sehingga menaikkan kecepatan reaksi reduksi oksidasi satu tingkat atau lebih. Diketahui pula bahwa kation logam alkali mempengaruhi adsorpsi hidrogen pada elektroda Pt(III) yang dimodifikasi dengan sianida, yang disebabkan oleh interaksi non-kovalen pada lapisan ganda elektrik, di antara anion atau dipole tertentu yang teradsorpsi dan kation logam alkali. Penelitian sistematis terhadap pengaruh konsentrasi kation logam alkali memungkinkan dikembangkannya model sederhana, yang menyerupai pengamatan eksperimental secara akurat, serta memungkinkan pemahaman akan kecenderungan dalam hal kekuatan interaksi dari M^+ dengan CN_{ad}^- ketika berpindah dari Li^+ ke Cs^+ , demikian juga pemahaman akan penyimpangan yang mungkin terjadi. Penelitian juga menunjukkan bahwa model sederhana ini dapat menjelaskan terjadinya pergeseran *super-Nernstian* pada keseimbangan potensial perpindahan pasangan proton-elektron. Hal ini menunjukkan bahwa model ini secara umum dapat diaplikasikan untuk menerangkan pengaruh kation secara kuantitatif terhadap sifat lapisan ganda elektrik. Pengaruh kation logam alkali terhadap beberapa reaksi elektrokatalitik yang baru-baru ini diterbitkan, harus dijumpai oleh interaksi antara kation-kation ini dan spesies yang teradsorpsi secara kimia, dan, karena interaksi ini diterangkan secara memadai dan kuantitatif oleh model yang kami kembangkan, kami harap model ini juga berguna untuk menerangkan, menjelaskan dan memanfaatkan pengaruh-pengaruh tersebut.

Keywords: *atomic-ensemble effects, cyanide-modified Pt(111), electrocatalysis, non-covalent interactions, single-crystal electrodes*

Introduction

Among all the challenges faced by humankind in the 21st century, generating enough energy to keep our greatly energy-consuming modern societies functioning while causing a minimum impact on the natural environment is probably the central and most important one. Electrochemical energy conversion and storage offers high theoretical efficiency because it can escape the limitations imposed by the second law of thermodynamics to the efficiency of a thermal engine. However, the actual efficiency of an electrochemical device is directly associated with the kinetics of the electron-transfer reactions occurring at the anode and cathode. Thus, a strong link is created between electrochemical science and technology and catalysis. Electrocatalysis is the science and art of finding a material on which the electrochemical reaction of interest can occur at the fastest rate possible. Eventually, an efficient electrochemical device is created.

Electrocatalysis, like heterogeneous catalysis, involves the interaction of reactants, products and intermediates with the surface of the catalytic material, as the breaking and forming of bonds is necessary to transform the reactants into new chemical species. The rate at which an elementary reaction step proceeds on the surface of a given catalyst not only depends on the strength of these interactions with the catalyst surface (generally considered as electronic effects) but also on the availability of specific atomic groupings that can provide the number of surface atoms necessary for chemisorption and act as active sites for a reaction or a reaction step (atomic ensemble effects).

Another effect that has traditionally been neglected is that of electrolyte cations or generally of any species in the electrolyte that does not form strong covalent chemical bonds with the atoms of the catalyst surface. However, cations can become attached to the electrode surface through non-covalent interactions (e.g., hydrogen bonds, ionic bonds, van der Waals forces, and hydrophobic interactions, which do not involve the sharing of pairs of electrons [1,2]) with chemisorbed species. Thus, the structure and the properties of the interface are affected, and the processes occurring at the electrochemical double layer are influenced as has been shown for some important electrocatalytic processes, such as the methanol oxidation reaction (MOR) [3] and the oxygen reduction reaction (ORR) [3,4].

This brief review offers an overview of recent works in my group using model cyanide-modified Pt(111) electrodes to achieve a deeper understanding of the atomic ensemble effects and non-covalent interactions at the electrode–electrolyte interface.

Cyanide-modified Pt(111): a peculiar surface. Saturated, irreversibly adsorbed cyanide adlayers can be formed on Pt(111) upon immersion in a cyanide-containing solution [5-9]. Infrared studies on cyanide adsorbed on Pt(111) electrodes have consistently found a single vibrational band corresponding to the stretching vibration of a CN group adsorbed on top of a platinum atom through its carbon end [5,6,8,9]. Hubbard and co-workers [7] showed using low-energy electron diffraction (LEED) that saturated, irreversibly adsorbed cyanide adlayers on Pt(111) formed an ordered $(2\sqrt{3} \times 2\sqrt{3})R30^\circ$ structure that resists electrode emersion and transfer into an ultrahigh vacuum (UHV) chamber. The same structure was observed later using electrochemical scanning tunneling microscopy (EC-STM) in cyanide-free alkaline solutions [9] and in cyanide-containing acidic and alkaline solutions [10]. The $(2\sqrt{3} \times 2\sqrt{3})R30^\circ$ structure consists of hexagonally packed hexagons, each containing six CN groups bonded linearly to a hexagon of Pt atoms through their carbon ends (Figure 1). The Pt atoms around the CN hexagons remain uncovered and lie at the bottom of one-atom-wide troughs. The platinum atom at the center of the hexagon also remains uncovered, thereby yielding a coverage by CN_{ad} of 0.5 ML.

As shown in Figure 1, cyanide-modified Pt(111) does not contain any sites composed of three contiguous platinum atoms. All the threefold-hollow adsorption sites have disappeared from the Pt(111) surface upon the formation of the cyanide $(2\sqrt{3} \times 2\sqrt{3})R30^\circ$ structure, thus fulfilling one of the conditions (removing only one

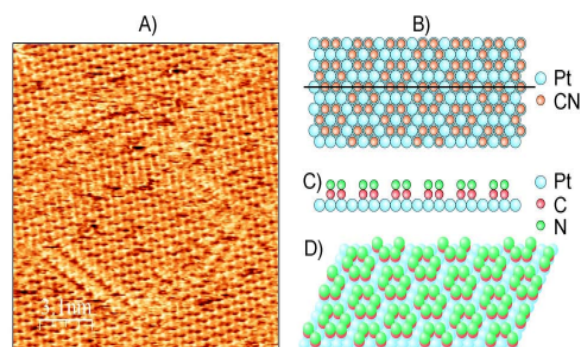


Figure 1. a) STM image ($16 \times 16 \text{ nm}^2$) of a Cyanide-modified Pt(111) electrode in $0.1 \text{ M HClO}_4 + 0.05 \text{ M KClO}_4$ at $E = 0.65 \text{ V}$ vs. RHE Showing the $(2\sqrt{3} \times 2\sqrt{3})R30^\circ$ Structure Adopted by the Adsorbed Cyanide. $U_T = 0.37 \text{ V}$ (Tip Negative); $I_T = 2 \text{ nA}$. b) Ball Model (Top View) of the $(2\sqrt{3} \times 2\sqrt{3})R30^\circ$ Structure Adopted by the Cyanide Adlayer on Pt(111). The Blue Balls Correspond to the Pt Atoms, and the Orange Balls Correspond to Irreversibly Adsorbed CN Groups. c) Cross-section of the $(2\sqrt{3} \times 2\sqrt{3})R30^\circ$ Structure along the Black Line in (b). d) Ball Model (Perspective) of the $(2\sqrt{3} \times 2\sqrt{3})R30^\circ$ Structure Adopted by the Cyanide Adlayer on Pt(111)

of the several kinds of sites present on the surface) required for studying atomic ensemble effects using the site-knockout strategy [11]. The other condition, which requires the electronic properties of the free platinum atoms not bonded to the CN groups to remain unaltered or only negligibly affected, is also fulfilled as we will show below.

Both the underpotential-deposited hydrogen (H_{upd} , i.e., hydrogen adsorbed at potentials more positive than the equilibrium potential for the hydrogen evolution reaction) and the adsorbed OH (OH_{ad}) regions are shifted in the positive direction in a cyanide-modified Pt(111) electrode compared with an unmodified Pt(111) (Figure 2). The observed potential shift implies that the ΔG^0 of H_{upd} and OH_{ad} at $\theta = 0$ are approximately 19 kJmol^{-1} more negative and approximately 24 kJmol^{-1} more positive, respectively, than that of an unmodified Pt(111)[12]. This result could be an indication of an electronic disturbance of the platinum atoms that remain

uncovered by CN on a cyanide-modified Pt(111) electrode. However, the weakening of the Pt- OH_{ad} can be most simply understood as being due to the electrostatic through-space repulsive interactions between the electronegative cyanide adlayer and the large negative dipole associated with OH_{ad} [4]. Regarding the increase in ΔG^0 of H_{upd} , we have recently shown that it is due to the formation of $(CN_{\text{ad}})_x\text{-H}$ clusters [13]. The formation of adsorbed hydrogen isocyanide (CNH_{ad}) was also argued by Schardt et al. [14] to explain the effect of pH on the amount of Cs^+ retained on the surface of a cyanide-modified Pt(111) electrode after immersion in a 0.1 mM CsCl solution. The formation of $(CN_{\text{ad}})_x\text{-H}$ clusters (where x must decrease with decreasing potential within the H_{upd} region) can also explain the change in the Stark tuning rate of the CN stretching frequency of a cyanide-modified Pt(111) electrode occurring at potentials more negative than 0.6V vs. RHE (coinciding with the onset

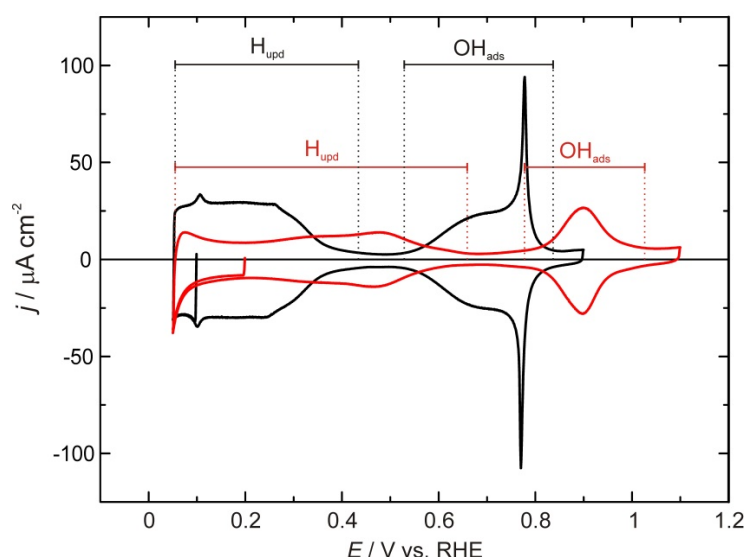


Figure 2. Cyclic Voltammogram of a Pt(111) (Black Line) and a Cyanide-modified Pt(111) (Red Line) Electrode in 0.1 M HClO_4 . Scan Rate: 50 mVs^{-1} . Source: Reference [11]

Table 1. Adsorption Energy (E_{ads}), Structural Parameters, and Mulliken Charges for the CN Radical Adsorbed *On-top* on Pt(111) at Low Coverage, and for the H Atom Adsorbed on the Nitrogen Atom of the CN (Pt(111)-CNH) and at a Pt Site Intermediate between *Bridge* and *Hcp-hollow* (NC-Pt(111)-H) in the Presence of a Low Coverage of CN_{ad}

Structure	E_{ads}/eV		Atomic distances / nm			Mulliken charges	
Pt(111)-CN ^{a)}	CN: -3.59		Pt-C: 0.194	C-N: 0.120		CN: -0.20	
Pt(111)-CNH ^{b)}	CNH: -1.86	H: -0.92	Pt-C: 0.189	C-N: 0.119	N-H: 0.101	CN: +0.38	H: -0.14
NC-Pt(111)-H ^{c)}	CN: -3.54	H: -0.55	Pt-C: 0.194	C-N: 0.120	Pt-H: 0.100	CN: -0.23	H: -0.20

^{a)} CN adsorbed *on-top* of a Pt(111) atom, $\theta = 1/9$. ^{b)} CNH adsorbed *on-top* of a Pt(111) atom, $\theta = 1/9$ (Figure 7B); the value given for CNH in column two corresponds to the E_{ads} of a CNH molecule on Pt(111) calculated with Eq. 6 in reference [13], and the value given for H corresponds to E_{ads} of an H atom on the N atom of an adsorbed CN moiety calculated with Eq. 5 in reference [13]. ^{c)} CN and H adsorbed *on-top* and at a site intermediate between *bridge* and *hcp-hollow*, respectively (Figure 7C in reference [13]); the value given for CN in column two corresponds to the E_{ads} of a CN radical on Pt(111) calculated with Eq. 1 in reference [13], and the value given for H corresponds to E_{ads} of an H atom on a CN-free Pt atom ($\theta_{\text{H}} = 1/9$) of a Pt(111) surface covered by 1/9 ML of CN calculated with Eq. 4 in reference [13].

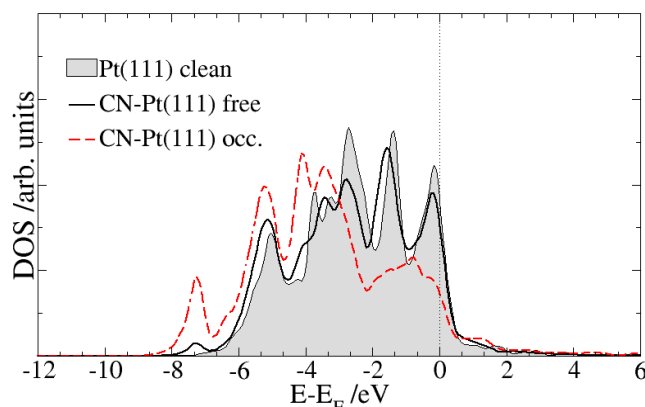


Figure 3. DOS of the d Band Projected on the Surface Atoms of a Clean Pt(111) and of a Cyanide-modified Pt(111) Surface with the Experimentally Observed ($2\sqrt{3} \times 2\sqrt{3}$)R30° Structure. For the Cyanide-Modified Pt(111) Surface, Pt Free Atoms (Not Bonded to Adsorbed Cyanide) are Distinguished from the Pt Atoms Directly Bonded to CN (Pt Occupied)

of H_{upd} formation) [5,15] and the incomplete blocking of hydrogen adsorption after adsorption of CO to saturation on a cyanide-modified Pt(111) electrode [15-17].

The most solid proof of the lack of electronic effects on cyanide-modified Pt(111) electrodes, though, is provided by density functional theory (DFT) calculations of the density of states (DOS) and hydrogen adsorption energies on clean Pt(111) and cyanide-modified Pt(111) surfaces [13, 18]. As shown in Figure 3, the DOS of the Pt atoms directly bonded to CN_{ad} is shifted to lower energies as expected for strong bonding, but the DOS of the atoms that are not bonded to CN_{ad} remains similar to that of the Pt atoms on the clean (111) surface. Similarly, as shown in Table 1, the adsorption energy of hydrogen on a cyanide-free Pt atom of a cyanide-modified Pt(111) is identical to that of hydrogen on an equivalent site of a Pt(111) surface within the error typical of DFT calculations. Furthermore, the transfer of a proton and an electron to the N atom of a CN group is clearly favored over adsorption on the cyanide-free atoms of a cyanide-modified Pt(111) surface.

Atomic ensemble effects on the electrocatalytic oxidation of C1 organic fuels and on the ORR.

Contrary to what is observed on Pt electrodes in general and on Pt(111) electrodes in particular, the cyclic voltammogram (CV) of a cyanide-modified electrode in a methanol-containing perchloric acid solution (Figure 4a) shows no change in the hydrogen adsorption region compared with the CV in the absence of methanol, and nearly no hysteresis occurs between the positive- and the negative-going sweeps [19]. These are two clear indications that no adsorbed CO is formed on the surface of the cyanide-modified Pt(111) electrode, as confirmed using infrared reflection-absorption spectroscopy (IRRAS) (Figure 4b) and later using differential electrochemical mass spectrometry (DEMS) [15]. These facts, along with the clear observation by IRRAS of CO_2 formation during methanol electro-

oxidation on cyanide-modified Pt(111) electrodes (Figure 4b, left panel), are a clear proof that a minimum of three contiguous Pt atoms (a trigonal site) is required for methanol dehydrogenation to adsorb CO, whereas two adjacent Pt atoms suffice for complete electrooxidation to CO_2 through the direct path. A similar conclusion was reached on the dehydration of formic acid [15]. Neurock et al. found the same result using DFT calculations [20].

The effect of removing the trigonal sites from the surface of a Pt(111) electrode on the ORR is even more dramatic. Figure 5 shows the polarization curves obtained using a rotating disc electrode (RDE) in O_2 -saturated 0.1 M $HClO_4$, 0.05 M H_2SO_4 , and 0.05 M H_3PO_4 solutions. In 0.1 M $HClO_4$, barely any difference can be observed between the activity of Pt(111) and that of a cyanide-modified Pt(111) electrode. This result is expected because perchlorate adsorbs only weakly, at the most, on Pt, and it is consistent with the idea that CN_{ad} acts simply as an inert site blocker without affecting the electronic properties of platinum. On the contrary, a 25-fold and a 10-fold increase in the activity for the ORR (measured at 0.9 V) is observed for cyanide-modified Pt(111) electrodes in 0.05 M H_2SO_4 and 0.05 M H_3PO_4 , respectively [4]. This finding can be attributed to the suppression of the trigonal sites necessary for the specific adsorption of the anions present in sulfuric and phosphoric acid solutions.

Quantitative description of interfacial non-covalent interactions and interfacial proton-coupled electron transfer (PCET).

Any cation in solution can be expected to interact with the negative end of the CN_{ad} dipole on the surface of a cyanide-modified Pt(111) electrode, blocking some of the CN_{ad} groups, which will not be available for the formation of $(CN_{\text{ad}})_x-H$ clusters, and provoking a change in the shape and/or position of the hydrogen adsorption region in the CV of cyanide-modified Pt(111) electrodes. This effect is illustrated in

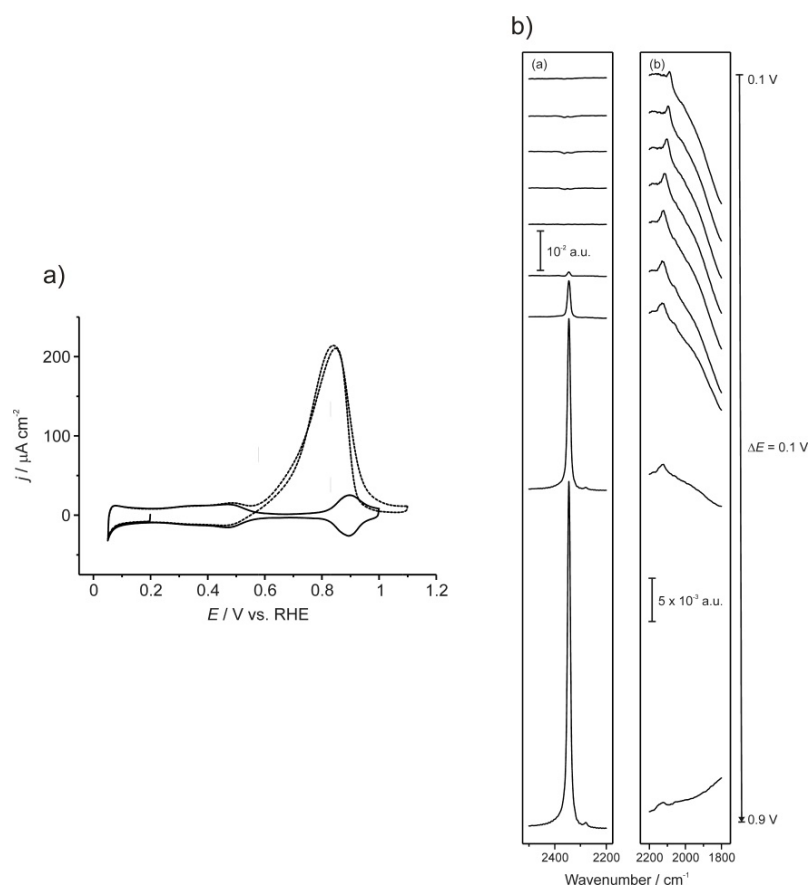


Figure 4. a) Cyclic Voltammogram at 50 mVs^{-1} of a Cyanide-modified Pt(111) Electrode in $0.1 \text{ M HClO}_4 + 0.2 \text{ M CH}_3\text{OH}$ (Dashed Line). The Scan Starts at 0.20 V in the Negative Direction. The Solid Line is the Cyclic Voltammogram of the Cyanide-modified Pt(111) in the Blank Electrolyte. b) FTIR Spectra at Increasing Potentials of the Cyanide-modified Pt(111) Electrode in $0.1 \text{ M HClO}_4 + 0.2 \text{ M CH}_3\text{OH}$. The Spectra in the Frequency Region between 2500 and 2200 cm^{-1} (left) were Calculated using the Spectrum at 0.05 V as Reference, and the Spectra in the Frequency Regions between 2200 and 1800 cm^{-1} (Right) were Calculated using the Spectrum at 1.30 V as Reference

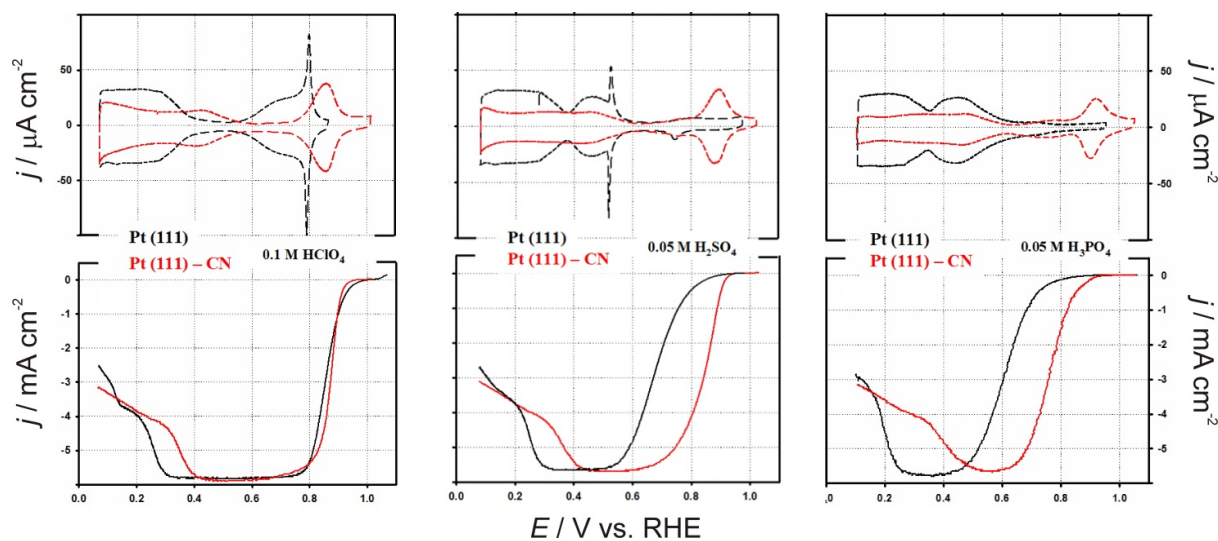


Figure 5. Cyclic Voltammograms in Ar-saturated Solutions (top) and Polarization Curves (bottom) in O_2 -saturated Solutions of a Pt(111) (Black Line) and a Cyanide-modified Pt(111) (Red Line) Electrode in 0.1 M HClO_4 (Left), $0.05 \text{ M H}_2\text{SO}_4$ (Center), and $0.05 \text{ M H}_3\text{PO}_4$ (Right). Scan Rate: 50 mVs^{-1} . The Polarization Curves were Recorded using an RDE at 1600 rpm

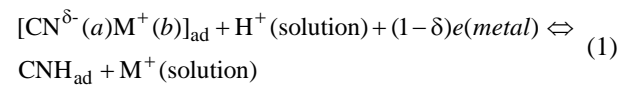
Figure 6a, which shows the variations observed in the CV of a cyanide-modified Pt(111) electrode as the concentration of K^+ increases. In Figure 6b, the potential at which a given coverage by $(CN_{ad})_x-H$ clusters has been achieved (i.e., at which a given adsorption charge has crossed the interface) is plotted as a function of the logarithm of the cation concentration for Li^+ , Na^+ , K^+ , and Cs^+ . As can be seen, at low concentrations, the peak potential remains constant in all the cases and equal to that in M^+ -free 0.1 M H_2SO_4 . Above a cation-dependent threshold concentration, the H_{upd} peak potential begins to deviate from the value in the absence of the cation. At high enough concentrations, the peak potential decreases linearly with the logarithm of the cation concentration. This behavior suggests that the cations are retained on the surface as $(CN_{ad})_x-M^+$ clusters in equilibrium with M^+ in the solution.

A similar effect is observed if the ionic strength and the cation concentration are kept constant and the pH is changed [21] as shown in Figure 7a for the case of Na^+ -containing solutions. Figure 7b shows plots of the potential (vs. the standard hydrogen electrode, SHE) at constant charge density (i.e., at constant θ_{CNH}) against pH. A line with a slope of -0.059 V is included as a guide to the eye. At all coverages, the potential shift is larger than the -0.059 V per pH unit expected for a PCET. The super-Nernstian contribution decreases slightly as θ_{CNH} approaches the maximum coverage possible, but at all θ_{CNH} , the shift of the equilibrium potential with pH remains far from the expected Nernstian value.

We developed a simple model that accounts for these two effects [18, 21]. The model is illustrated in Figure 8a, which shows a ball model of the structure of the cyanide-modified Pt(111) surface with cations adsorbed at sites surrounded by three CNs, as in the experimentally observed honeycomb structure [18]. Figure 8b shows a cross-section along the line in Figure 8a and a schematic representation of the electrode-electrolyte interface. The PCET occurs at plane a , which is defined by the position of the specifically adsorbed hydrogen acceptor/proton donor, namely, the N atom of CN_{ad}/CNH_{ad} . The presence of the cations interacting non-covalently with CN_{ad} defines a plane of maximum approach b , where the proton donor (H_3O^+ in acidic solutions and H_2O in alkaline solutions) or acceptor (H_2O in acidic solutions and OH^- in alkaline solutions) has to be transferred from the limit of the diffuse double layer (which, in concentrated solutions like the ones used here, coincides with the outer Helmholtz plane, OHP) before reaching a for the PCET to occur.

The assumptions made in the model are summarized as follows: a). The proton-coupled electron transfer corresponding to the electroadsorption of hydrogen on a cyanide-modified Pt(111) electrode does not take place

at the metal surface, where the electrostatic potential is ϕ_m , but at a plane a , which is somewhere between the metal surface and the OHP, where the electrostatic potential is ϕ_a ; b). In the presence of a cation in the solution, a cation layer in equilibrium with cations in the bulk electrolyte is anchored at plane b by the cyanide-modified Pt(111) electrode through electrostatic interactions. At high enough electrolyte concentrations, plane b can be assumed to coincide with the OHP. Therefore, the energy required to remove the cation from plane b contributes to ΔG of the hydrogen electroadsorption reaction; c). The hydrogen electroadsorption reaction may involve the transfer of less than one electron per proton transferred because of the polar nature of the Pt-CN surface bond. Together with the previous conditions, the hydrogen electroadsorption reaction to be considered is



d). The potential drop across the interface is linear. Consequently, the potential difference between plane a and the solution, ϕ^a is a fraction of the total potential drop across the interface, ϕ^m , given by $\phi^a = \omega_a \phi^m$, where $\omega_a = C_{m/OHP} / C_{a/OHP}$, where $C_{m/OHP}$ is the integral capacity of the electrical double layer, and $C_{a/OHP}$ is the integral capacity of the dielectric slab limited by plane a and the OHP (i.e., $0 \leq \omega_a \leq 1$). With the assumptions above, the equilibrium condition for Reaction (1) is

$$\phi^m = f(\theta_{CNH}) + \frac{RT}{[1-\delta(1-\omega_a)]F} \ln \frac{a_{H^+}}{1 + K_{as} a_{M^+}} \quad (2)$$

With

$$f(\theta_{CNH}) = \frac{RT}{[1-\delta(1-\omega_a)]F} \left(\frac{-\Delta G_{H^+/H}^0}{RT} + \ln \frac{1-\theta_{CNH}}{\theta_{CNH}} \right)$$

where $-\Delta G_{H^+/H}^0 = \mu_{CN}^0 + \mu_{H^+}^0 + (1-\delta)\mu_e^0 - \mu_{CNH}^0$. a_{H^+} is the activity of H^+ in the bulk solution, $K_{as} = \exp(-\Delta G_{as}^0 / RT)$ is the association constant of the non-reductive adsorption of M^+ on the cyanide adlayer at $\phi^m = 0$ (with $-\Delta G_{as}^0 = \mu_{CN}^0 + \mu_{M^+}^0 - \mu_{CNM}^0$), and a_{M^+} is the activity of M^+ in the bulk solution. The remaining terms have their usual meaning.

Two limiting cases are analyzed: The pH is kept constant and the cation concentration varies as in the experiments illustrated in Figure 6. Under these conditions, Equation (2) becomes

$$\phi^m = f'(\theta_{CNH}) - \frac{RT}{[1-\delta(1-\omega_a)]F} \ln(1 + K_{as} a_{M^+}) \quad (3)$$

where

$$f'(\theta_{\text{CNH}}) = \frac{RT}{[1-\delta(1-\omega_a)]F} \left(\frac{-\Delta G_{\text{H}^+/\text{H}}^0}{RT} + \ln \frac{1-\theta_{\text{CNH}}}{\theta_{\text{CNH}}} + \ln a_{\text{H}^+} \right)$$

Equation (3), which is equivalent to Equation (2) in reference [18], predicts a constant equilibrium potential for $K_{as} a_{\text{M}^+} \ll 1$. A fit of the experimental results to Equation (2) allows to obtain $[1-\delta(1-\omega_a)]$ and K_{as} . Table 2 lists the values obtained for the cases of Li^+ , Na^+ , K^+ , and Cs^+ , together with their standard Gibbs free energy of hydration and their ionic radii.

K_{as} would be expected to increase with decreasing cation radius. However, by contrast, it increases strongly from Li^+ to K^+ and decreases from K^+ to Cs^+ . This observation cannot be explained only by the decrease in the hydration energy with the increasing cation radius, and it suggests that additional stability of the $(\text{CN}_{\text{ad}})_x\text{M}^+$ cluster is provided by an optimal fit of the cation into a cavity formed by the CN groups, similar to some [2]-cryptate inclusion complexes formed by macrobicyclic ligands and alkali metals [22]. The size of the cavity formed by the CN groups must be

close to the atomic diameter of Pt (2.77 Å), and K^+ must fit well inside it. Although Cs^+ has a lower hydration energy than K^+ , it is too large to fit in the cavity, and therefore its K_{as} is smaller.

The cation size also affects the value of $[1-\delta(1-\omega_a)]$. Smaller cations can approach closer to plane *a* to yield a large $C_{\text{a/OHP}}$, a small ω_a , and a small $[1-\delta(1-\omega_a)]$. Again, K^+ deviates from the expected trend because of the excellent match between its ionic radius and the size of the $(\text{CN}_{\text{ad}})_3$ cavity.

The cation concentration is kept constant and the pH is changed similar to the experiments illustrated in Figure 6. Under these conditions, Equation (2) becomes

$$\varphi^{\text{m}} = f'(\theta_{\text{CNH}}) - \frac{RT}{[1-\delta(1-\omega_a)]F} \ln a_{\text{H}^+} \quad (4)$$

where

$$f'(\theta_{\text{CNH}}) = \frac{RT}{[1-\delta(1-\omega_a)]F} \left(\frac{-\Delta G_{\text{H}^+/\text{H}}^0}{RT} + \ln \frac{1-\theta_{\text{CNH}}}{\theta_{\text{CNH}}} - \ln(1 + K_{as} a_{\text{M}^+}) \right)$$

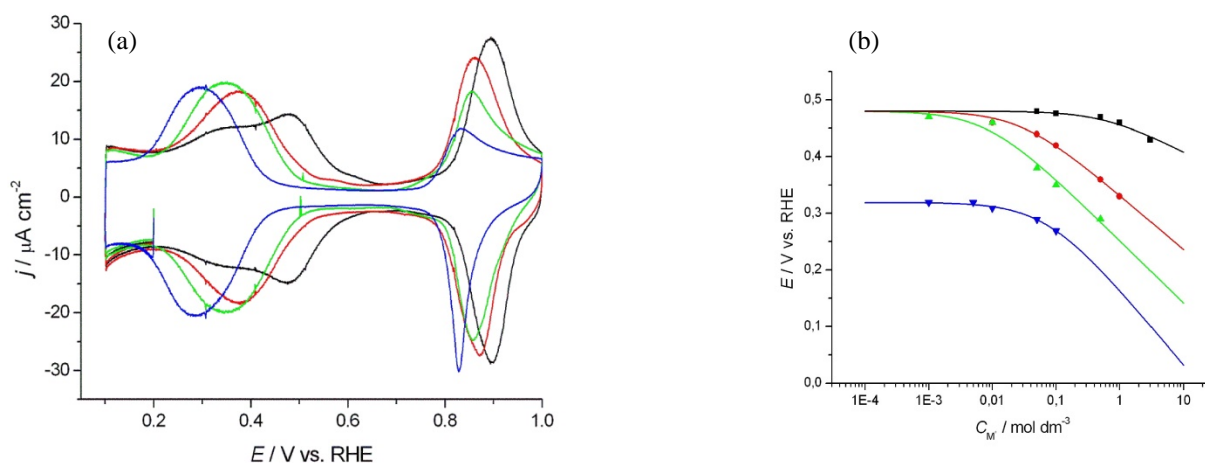


Figure 6. a) Cyclic Voltammogram of the Cyanide-modified Pt(111) in 0.1 M HClO_4 (H_2SO_4) + x KClO_4 (K_2SO_4): $x = 0$ M (Black), 0.05 M (Red), 0.1 M (Green), and 0.5 M (Blue). Scan Rate: 50 mV s^{-1} . b) Semilogarithmic Plot of the Dependence on the Cation Concentration of the Peak Potential for Hydrogen Adsorption on the Cyanide-modified Pt(111) Electrodes in 0.1 M H_2SO_4 or HClO_4 as Obtained from Cyclic Voltammograms at 50 mV s^{-1} . Black Squares: Li^+ ; Red Circles: Na^+ ; Green up Triangles: K^+ ; Blue Down Triangles: Cs^+ . The Lines Correspond to the fit of the Experimental Data to Equation (3)

Table 2. Equilibrium Constants for the Formation of the $(\text{CN}_{\text{ad}})_3\text{-M}^+$ Clusters (K_{as}) and Apparent Number of Electrons Crossing the Interface per Every H^+ Transferred, $[1-\delta(1-\omega_a)]$, as Obtained from the Fit of the Experimental Data in Figure 6b to the Model Described by Eq. (3). The Last Two Columns Show the Gibbs Energy of Hydration (ΔG^0) and the Ionic Diameter of the Cations

	K_{as} / M^{-1}	$[1-\delta(1-\omega_a)]$	$\Delta G^0 / \text{eV}^{\text{a}}$	Ionic diameter / Å ^a
Li^+	0.24 ± 0.07	0.28 ± 0.07	-5.3	1.56
Na^+	34 ± 6	0.61 ± 0.04	-4.3	1.96
K^+	120 ± 50	0.54 ± 0.08	-3.5	2.66
Cs^+	31 ± 11	0.8 ± 0.1	-2.9	3.30

^aValues taken from reference [22]

Even in the absence of a cation, a super-Nernstian shift of the hydrogen electroadsorption process will occur if the chemisorption bond between Pt and CN_{ad} is polar.

Above a K_{as} -dependent threshold concentration, the presence of the cation (i) shifts $f'(\theta_{\text{CNH}})$ negatively by

$$\frac{RT}{[1 - \delta(1 - \omega_a)]F} \ln(1 + K_{\text{as}} a_{\text{M}^+}) \text{ V (i.e., even if } \delta = 0, \text{ the}$$

PCET in MOH solutions will shift by $-\frac{RT}{F} \ln(1 + K_{\text{as}} a_{\text{M}^+})$. V in the RHE when compared with HClO_4 or H_2SO_4 solutions) and (ii) separates plane a from the OHP.,

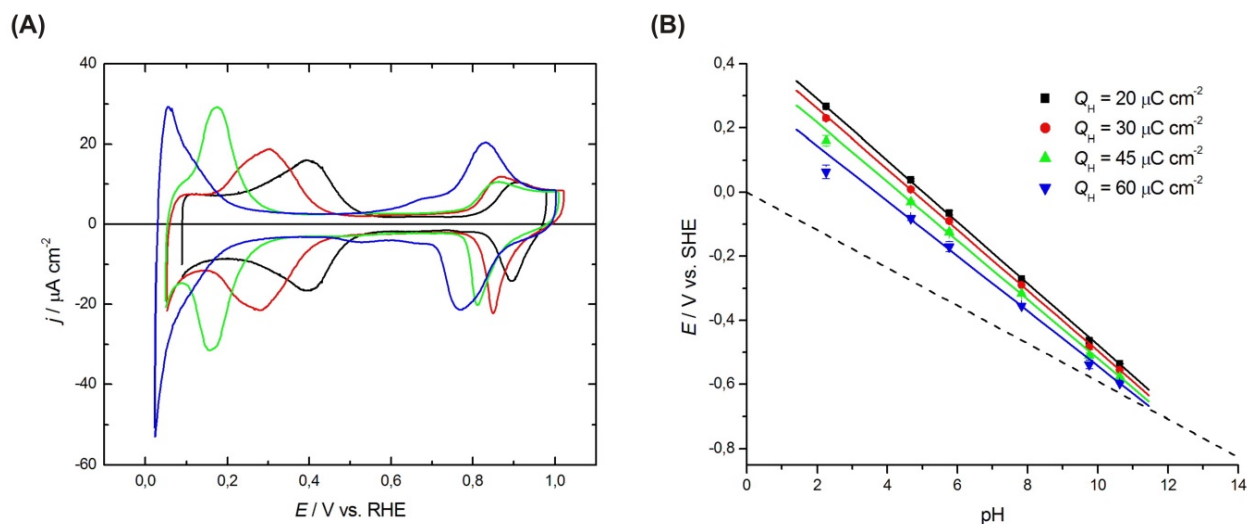


Figure 7. a) Cyclic Voltammograms at 50 mV s^{-1} of a Cyanide-modified Pt(111) Electrode in Phosphate-buffer Solutions of pH 2 (Black Line), 4 (Red Line), 8 (Green Line), and 11 (Blue Line). Adequate Amounts of NaClO_4 were Added to the Solutions to Keep the Ionic Strength and the Concentration of Na^+ Constant. b) Potential (in the SHE Scale) vs. pH at Constant Hydrogen Adsorption Charge Densities of $20 \text{ } \mu\text{C cm}^{-2}$ (Black), $30 \text{ } \mu\text{C cm}^{-2}$ (Red), $45 \text{ } \mu\text{C cm}^{-2}$ (Green), and $60 \text{ } \mu\text{C cm}^{-2}$ (Blue). For the Sake of Comparison, a Line with a Slope of -0.059 V Corresponding to the Nernstian Behavior Expected for a PCET is also Included (Dashed Line)

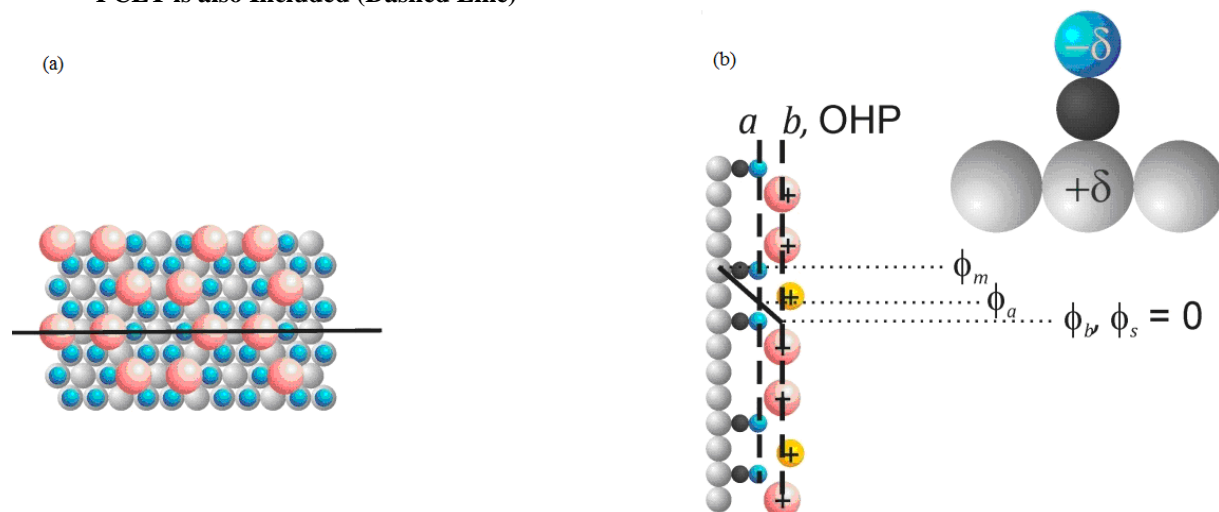


Figure 8. a) Ball Model of the Structure of Cyanide-modified Pt(111) with Cations (Red Balls) Interacting Non-covalently with CN_{ad} (Blue Balls) to Form the Experimentally Observed Honeycomb Structure.[18] The Gray Balls Correspond to the Substrate Pt Atoms. b) Cross-section along the Solid Line in (a) and the Schematic Representation of the Electrical Double Layer, which Indicates the Location of the Plane of the Proton-electron Transfer, a , and of the Plane of Maximum Approach of Cations and Protons, b (which, for the Sake of Simplicity, we have Made to Coincide with the OHP; See Text). The Black Balls Correspond to the Carbon Atoms, and the Blue Balls Correspond to the Nitrogen Atoms of the CN Groups. The Yellow Balls Correspond to Hydrated Protons. The Inset Illustrates the Polar Nature of the Chemisorption Bond

making $\omega_a \neq 0$ and decreasing the slope of the pH dependence. The increase in the hydrogen coverage as the potential is made more negative must also provoke an increase in the separation between plane a and the OHP, which provokes an increase in ω_a and a decrease in the super-Nernstian contribution (see Figure 7). As predicted by Equations (3) and (4), the same value of $[1-\delta(1-\omega_a)] = 0.61$ is obtained from both kinds of experiments for Na^+ at a constant charge of $20 \mu\text{C cm}^{-2}$ more negative than expected from a merely Nernstian shift [23, 24]. This has been suggested to be the reason for the higher electrocatalytic activity of Pt and other metals in alkaline media toward the oxidation of some organic molecules compared with acidic environments [25-28]. Our work provides an explanation for these phenomena.

Conclusions

We have shown that the site-knockout strategy enables us to study atomic ensemble effects in electrocatalytic reactions without interference of electronic effects. Atomic ensemble effects can be used to improve both the activity and the selectivity of an electrocatalyst.

Our work has also shown that cations can adsorb on the electrode surface as ion pairs form with specifically adsorbing anions. These electrostatic (or generally non-covalent) interactions, which can affect the properties of the electrode–electrolyte interface and therefore the processes occurring in this region including electrocatalytic reactions, are suitably described by the proposed simple model.

PCETs to specifically adsorbed anions exhibit a super-Nernstian shift with pH if the chemisorption bond is polar and if the plane at which the proton–electron transfer occurs does not coincide with the electrode surface. If above a cation-dependent threshold concentration, the presence in the electrolyte of cations other than H^+ can have a double effect: (i) cations provoke an additional negative shift of the PCET because of the additional energy required to remove the cation layer before the proton can access the plane at which hydrogenation occurs, and (ii) they affect the magnitude of the super-Nernstian shift by separating the plane of hydrogenation and the OHP.

In addition to the most usually considered electronic effect, atomic ensemble effects and the electrolyte composition can be used to tune the catalytic activity of electrode–electrolyte interfaces.

Acknowledgments

This brief review is based on a Keynote Lecture delivered at the Materials Chemistry for Energy and the Environment (MCEE) Workshop held in Bogor,

Indonesia, from January 26–29, 2016 and funded by the British Council and the Royal Society of Chemistry within the Newton-Fund Researcher Links Program.

References

- [1] Lodish, H., Berk, A., Zipursky, S.L., Matsudaira, P., Baltimore, D., Darnell, J. 2000. *Molecular Cell Biology*, 4th ed. W.H. Freeman. New York. Section 2.2, <http://www.ncbi.nlm.nih.gov/books/NBK21726>.
- [2] Schalley, C.A. 2007. Introduction. In Schalley, C.A. (ed.), *Analytical Methods in Supramolecular Chemistry*. Wiley-VCH Verlag GmbH & Co. KGaA. Weinheim. pp. 1-16.
- [3] Strmcnik, D., Kodama, K., van der Vliet, D., Greeley, J., Stamenkovic, V.R., Marković, N.M. 2009. The role of non-covalent interactions in electrocatalytic fuel-cell reactions on platinum. *Nat. Chem.* 1(6): 466-472, <http://dx.doi.org/10.1038/nchem.330>.
- [4] Strmcnik, D., Escudero-Escribano, M., Kodama, K., Stamenkovic, V.R., Cuesta, A., Marković, N.M. 2010. Enhanced electrocatalysis of the oxygen reduction reaction based on patterning of platinum surfaces with cyanide. *Nat. Chem.* 2(10): 880-885, <http://dx.doi.org/10.1038/nchem.771>.
- [5] Huerta, F., Morallón, E., Quijada, C., Vázquez, J.L., Aldaz, A. 1998. Spectroelectrochemical study on CN- adsorbed at Pt(111) in sulphuric and perchloric media. *Electrochim. Acta* 44(6-7): 943-948, [http://dx.doi.org/10.1016/S00134686\(98\)00197-2](http://dx.doi.org/10.1016/S00134686(98)00197-2).
- [6] Huerta, F., Morallón, E., Vázquez, J.L. 1999. Structural effects of adsorbed CN adlayers on the co-adsorption of OH- at the Pt(111) surface in sulfuric acid medium. *Surf. Sci.* 431(1-3): L577-L581, [http://dx.doi.org/10.1016/S0039-6028\(99\)00580-4](http://dx.doi.org/10.1016/S0039-6028(99)00580-4).
- [7] Stickney, J.L., Rosasco, S.D., Salaita, G.N., Hubbard, A.T. 1985. Ordered ionic layers formed on platinum(111) from aqueous solutions. *Langmuir* 1(1): 66-71, <http://dx.doi.org/10.1021/la00061a009>.
- [8] Stuhlmann, C. 1995. Characterization of an electrode adlayer by in-situ infrared spectroscopy: cyanide on Pt(111). *Surf. Sci.* 335(0): 221-226, [http://dx.doi.org/10.1016/0039-6028\(95\)00420-3](http://dx.doi.org/10.1016/0039-6028(95)00420-3).
- [9] Stuhlmann, C., Villegas, I., Weaver, M.J. 1994. Scanning tunneling microscopy and infrared spectroscopy as combined in situ probes of electrochemical adlayer structure. Cyanide on Pt(111). *Chem. Phys. Lett.* 219(3-4): 319-324, [http://dx.doi.org/10.1016/0009-2614\(94\)87064-0](http://dx.doi.org/10.1016/0009-2614(94)87064-0).
- [10] Kim, Y.-G., Yau, S.-L., Itaya, K. 1996. Direct Observation of Complexation of Alkali Cations on Cyanide-Modified Pt(111) by Scanning Tunneling Microscopy. *J. Am. Chem. Soc.* 118(2): 393-400, <http://dx.doi.org/10.1021/ja9521841>.

- [11] Cuesta, A. 2011. Atomic Ensemble Effects in Electrocatalysis: The Site-Knockout Strategy. *ChemPhysChem* 12(13): 2375-2385, <http://dx.doi.org/10.1002/cphc.201100164>.
- [12] Cuesta, A., Escudero, M. 2008. Electrochemical and FTIRS characterisation of NO adlayers on cyanide-modified Pt(111) electrodes: the mechanism of nitric oxide electroreduction on Pt. *Phys. Chem. Chem. Phys.* 10(25): 3628-3634, <http://dx.doi.org/10.1039/B717396B>.
- [13] Escudero-Escribano, M., Soldano, G.J., Quaino, P., Zoloff Michoff, M.E., Leiva, E.P.M., Schmickler, W., Cuesta, Á. 2012. Cyanide-modified Pt(111): Structure, stability and hydrogen adsorption. *Electrochim. Acta* 82: 524-533, <http://dx.doi.org/10.1016/j.electacta.2012.02.062>.
- [14] Schardt, B.C., Stickney, J.L., Stern, D.A., Frank, D.G., Katekaru, J.Y., Rosasco, S.D., Salaita, G.N., Soriaga, M.P., Hubbard, A.T. 1985. Surface coordination chemistry of well-defined platinum electrodes: surface polyprotic acidity of platinum(111)(2). *Inorg. Chem.* 24(10): 1419-1421, <http://dx.doi.org/10.1021/ic00204a001>.
- [15] Cuesta, A., Escudero, M., Lanova, B., Baltruschat, H. 2009. Cyclic Voltammetry, FTIRS, and DEMS Study of the Electrooxidation of Carbon Monoxide, Formic Acid, and Methanol on Cyanide-Modified Pt(111) Electrodes. *Langmuir* 25(11): 6500-6507, <http://dx.doi.org/10.1021/la8041154>.
- [16] Huerta, F., Morallón, E., Vázquez, J.L. 2002. Voltammetric analysis of the co-adsorption of cyanide and carbon monoxide on a Pt(111) surface. *Electrochem. Commun.* 4(3): 251-254, [http://dx.doi.org/10.1016/S1388-2481\(02\)00271-0](http://dx.doi.org/10.1016/S1388-2481(02)00271-0).
- [17] Morales-Moreno, I., Cuesta, A., Gutiérrez, C. 2003. Accurate determination of the CO coverage at saturation on a cyanide-modified Pt(111) electrode in cyanide-free 0.5 M H₂SO₄. *J. Electroanal. Chem.* 560(2): 135-141, <http://dx.doi.org/10.1016/j.jelechem.2003.07.008>.
- [18] Escudero-Escribano, M., Zoloff Michoff, M.E., Leiva, E.P.M., Marković, N.M., Gutiérrez, C., Cuesta, Á. 2011. Quantitative Study of Non-Covalent Interactions at the Electrode-Electrolyte Interface Using Cyanide-Modified Pt(111) Electrodes. *ChemPhysChem* 12(12): 2230-2234, <http://dx.doi.org/10.1002/cphc.201100327>.
- [19] Cuesta, A. 2006. At Least Three Contiguous Atoms Are Necessary for CO Formation during Methanol Electrooxidation on Platinum. *J. Am. Chem. Soc.* 128(41): 13332-13333, <http://dx.doi.org/10.1021/ja0644172>.
- [20] Neurock, M., Janik, M., Wieckowski, A. 2009. A first principles comparison of the mechanism and site requirements for the electrocatalytic oxidation of methanol and formic acid over Pt. *Faraday Discuss.* 140: 363-378, <http://dx.doi.org/10.1039/B804591G>.
- [21] Wildi, C., Cabello, G., Zoloff Michoff, M.E., Vélez, P., Leiva, E.P.M., Calvente, J.J., Andreu, R., Cuesta, A. 2016. Super-Nernstian Shifts of Interfacial Proton-Coupled Electron Transfers: Origin and Effect of Non-Covalent Interactions. *J. Phys. Chem. C* 120(29): 15586-15592, <http://dx.doi.org/10.1021/acs.jpcc.5b04560>.
- [22] Lehn, J.M., Sauvage, J.P. 1975. Cryptates. XVI. [2]-Cryptates. Stability and selectivity of alkali and alkaline-earth macrobicyclic complexes. *J. Am. Chem. Soc.* 97(23): 6700-6707, <http://dx.doi.org/10.1021/ja00856a018>.
- [23] Burke, L.D., Lyons, M.E., Whelan, D.P. 1982. Influence of pH on the reduction of thick anodic oxide films on gold. *J. Electroanal. Chem.* 139(1): 131-142, [http://dx.doi.org/10.1016/0022-0728\(82\)85109-7](http://dx.doi.org/10.1016/0022-0728(82)85109-7).
- [24] Burke, L.D., Roche, M.B.C. 1983. The possible importance of hydrolysis effects in the early stages of metal surface electrooxidation reactions — With particular reference to platinum. *J. Electroanal. Chem.* 159(1): 89-99, [http://dx.doi.org/10.1016/S0022-0728\(83\)80316-7](http://dx.doi.org/10.1016/S0022-0728(83)80316-7).
- [25] Marković, N.M., Lucas, C.A., Rodes, A., Stamenković, V., Ross, P.N. 2002. Surface electrochemistry of CO on Pt(111): anion effects. *Surf. Sci.* 499(2-3): L149-L158, [http://dx.doi.org/10.1016/S0039-6028\(01\)01821-0](http://dx.doi.org/10.1016/S0039-6028(01)01821-0).
- [26] Marković, N.M., Ross Jr, P.N. 2002. Surface science studies of model fuel cell electrocatalysts. *Surf. Sci. Rep.* 45(4-6): 117-229, [http://dx.doi.org/10.1016/S0167-5729\(01\)00022-X](http://dx.doi.org/10.1016/S0167-5729(01)00022-X).
- [27] Spendelow, J.S., Goodpaster, J.D., Kenis, P.J.A., Wieckowski, A. 2006. Mechanism of CO Oxidation on Pt(111) in Alkaline Media. *J. Phys. Chem. B* 110(19): 9545-9555, <http://dx.doi.org/10.1021/jp060100c>.
- [28] Spendelow, J.S., Lu, G.Q., Kenis, P.J.A., Wieckowski, A. 2004. Electrooxidation of adsorbed CO on Pt(111) and Pt(111)/Ru in alkaline media and comparison with results from acidic media. *J. Electroanal. Chem.* 568: 215-224, <http://dx.doi.org/10.1016/j.jelechem.2004.01.018>.